**Supplementary information**

# A Multiscale Coarse-Grained Model to Predict the Molecular Architecture and Drug Transport Properties of Modified Chitosan Hydrogels

Ankush Singhal[1], John D. Schneible[2], Radina L. Lilova[2], Carol K. Hall[2,*], Stefano Menegatti[2,*], Andrea Grafmüller[1,*]

1. Department of Theory and Biosystems, Max Planck Institute for Colloids and Interfaces, Potsdam 14476, Germany.

2. Department of Chemical and Biomolecular Engineering, North Carolina State University, Raleigh, North Carolina 27695, United States.

* Corresponding authors e-mail: hall@ncsu.edu (C.K.H.), smenega@ncsu.edu (S.M.), and Andrea.Grafmueller@mpikg.mpg.de (A.G.)

## S.1 Complete set of bonded interaction for chitosan

In this study, the coarse-grained GlcN monomer (**Figure 1a – 1c**) comprises beads connected by three bonds, namely $A_i$-$B_i$, $A_i$-$C_i$, and $B_i$-$C_i$; the glycosidic bond connecting two GlcN monomers, , is described by is described by one bond, $C_i$-$A_{i+1}$, two angles ($A_i$-$C_{i-1}$-$B_{i-1}$ and $C_{i-1}$-$A_i$-$B_i$) and three dihedral potentials($A_i$-$B_i$-$C_i$-$A_{i+1}$, $B_{i-1}$-$C_{i-1}$-$A_i$-$B_i$, and $C_{i-1}$-$A_i$-$B_i$-$C_i$). In addition, two explicit non-bonded (1-3) intramolecular interactions ($A_i$-$A_{i+1}$ and $C_i$-$C_{i+1}$) and two non-bonded (1-4) intramolecular interactions ($B_i$-$B_{i+1}$ and $A_i$-$C_{i+1}$) were also applied.

To describe the chemical modifications, additional bonds, angles, and dihedrals were introduced as follows: acetyl modifications were modeled with one bead (M), one bond ($M_i$-$A_i$), one angle ($M_i$-$A_i$-$C_i$), two dihedrals ($M_i$-$A_i$-$B_i$-$C_i$ and $M_i$-$A_i$-$C_{i-1}$-$B_{i-1}$), two explicit non-bonded

(1-3) interactions ($M_i$-$B_i$ and $M_i$-$C_{i-1}$), and two explicit non-bonded (1-4) interactions ($M_i$-$A_{i-1}$ and $M_i$-$A_{i+1}$); butanoyl modifications were modeled with two beads (MA, which has the same bonded structure as M, and MB), two additional bonds ($MA_i$-$A_i$ and $MA_i$-$MB_i$), explicit (1-3) interaction ($MB_i$-$A_i$) and (1-4) interactions ($MB_i$-$B_i$, $MB_i$-$C_i$, and $MB_i$-$C_{i-1}$); similarly, heptanoyl modifications were modeled with three beads (MA, MB, and MC), three bonds ($MA_i$-$A_i$ and $MA_i$-$MB_i$, $MC_i$-$MB_i$), one more explicit (1-3) interaction ($MC_i$-$MA_i$), and one additional explicit (1-4) interaction ($MC_i$-$A_i$).

**S.2 Complete set of bonded interaction for Dox and Gem**

Dox was mapped to 11 CG beads using 9 distinct bead types, as shown in **Figure 1d**. Bonded interactions comprise 13 bonds (DA-DB, DA-DC1, DB-DC2, DC1-DC2, DC1-DD1, DC2-DD2, DD1-DE, DD2-DE, DE-DF, DD2-DG, DG-DH, DG-DI, and DH-DI), 4 angles (DC2-DD2- DG, DD1-DE-DF, DD2-DG-DH, and DE-DD2-DG), and 5 dihedrals (DC1-DD1-DD2-DG, DC2-DD2-DG-DH, DD2-DG-DH-DI, DF-DE-DD2-DG, and DE-DD2-DG-DH).

Gem was mapped to 4 distinct CG beads. The molecular geometry was described by four bonds (GA-GB, GB-GC, GA-GC and GC-GD) and two explicit 1-3 intra-molecular interactions (GA-GD and GB-GD).

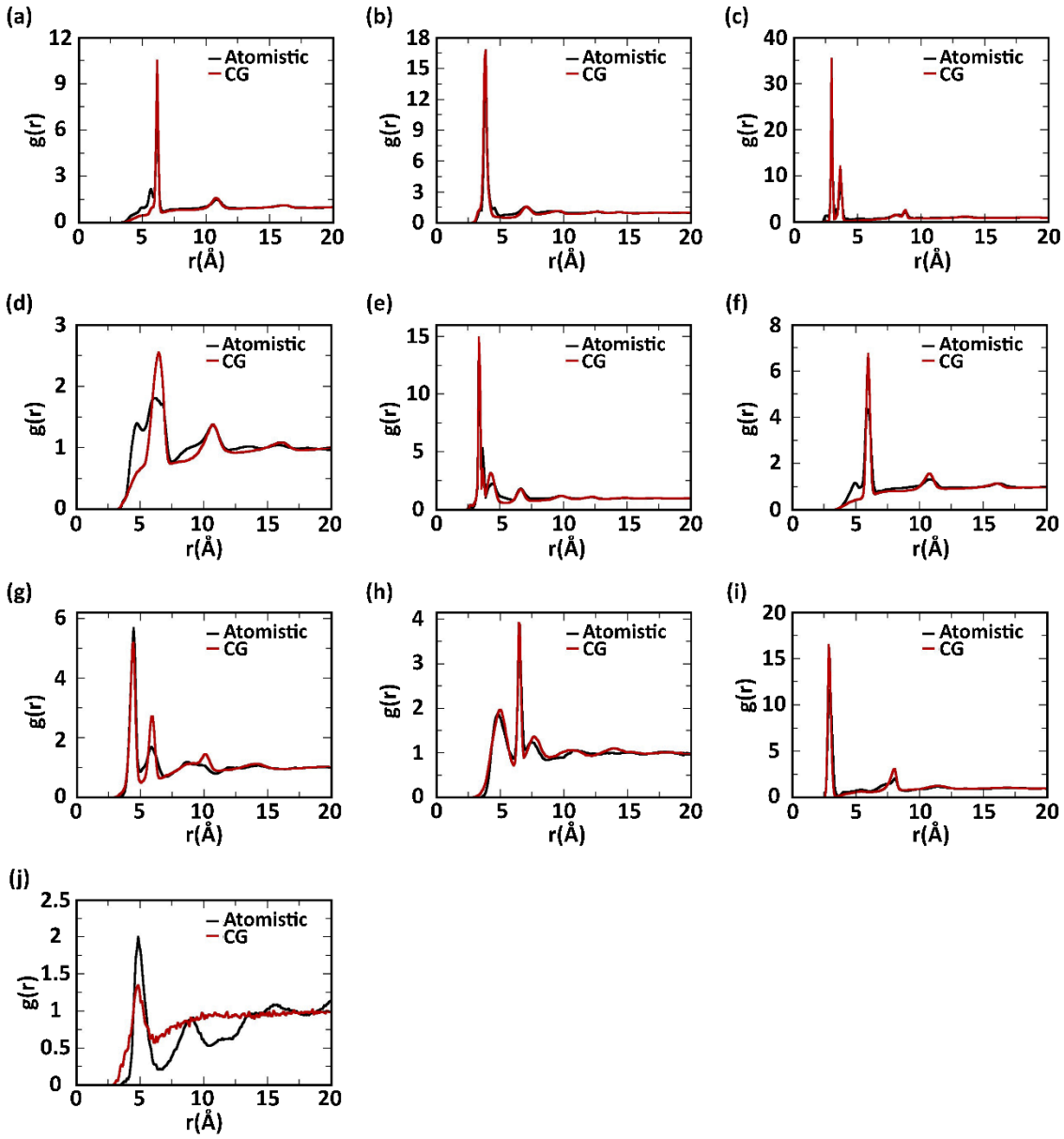


***Figure S1.*** *RDFs of the distance between CG beads* ***(a)*** *A-A,* ***(b)*** *A-B,* ***(c)*** *A-C,* ***(d)*** *B-B,* ***(e)*** *B-C,* ***(f)*** *C-C,* ***(g)*** *C-M,* ***(h)*** *B-M,* ***(i)*** *A-M, and* ***(j)*** *M-M in acetyl-chitosan obtained from atomistic (black) and CG (red) simulations.*

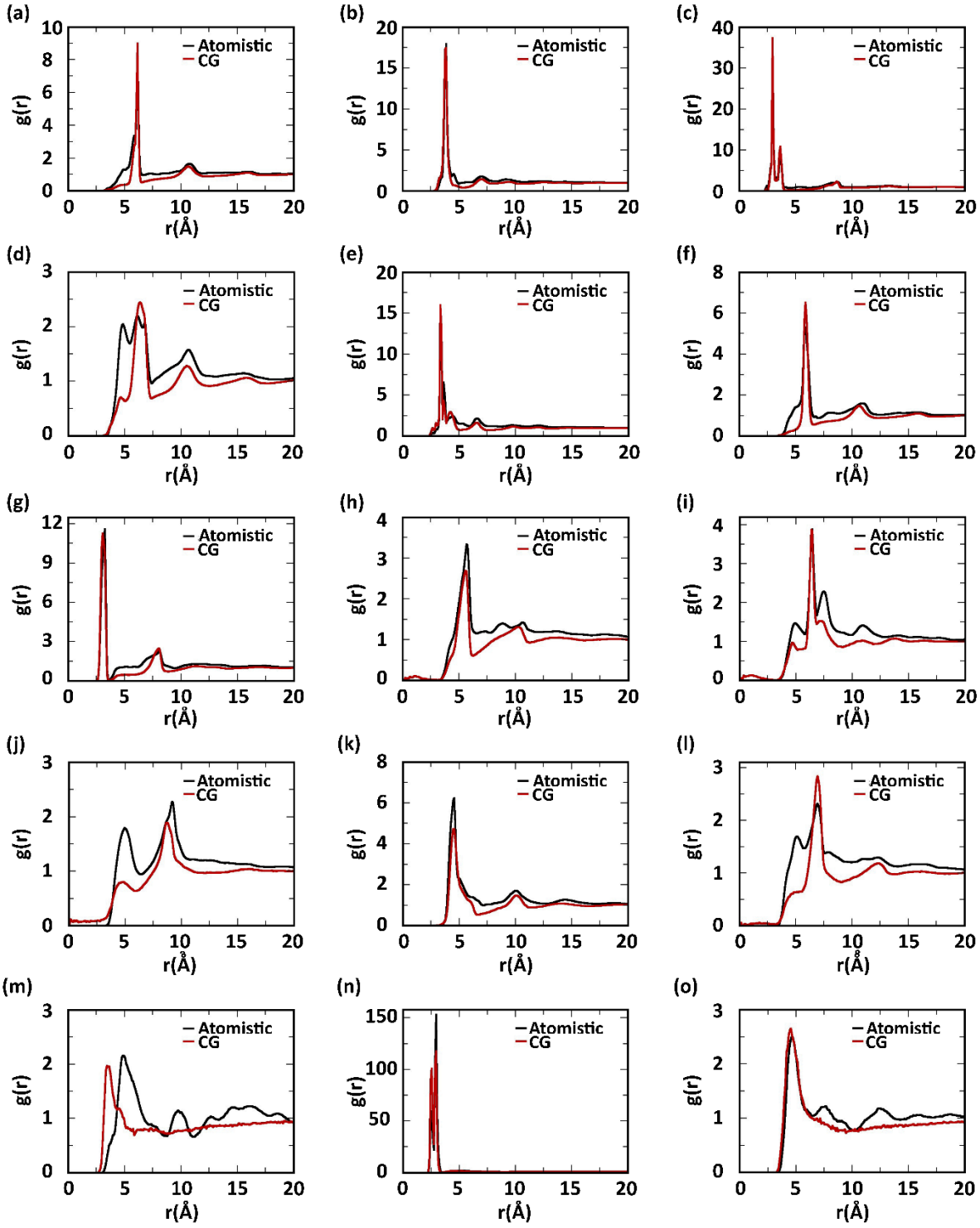


***Figure S2.*** *RDFs of the distance between CG beads* ***(a)*** *A-A,* ***(b)*** *A-B,* ***(c)*** *A-C,* ***(d)*** *B-B,* ***(e)*** *B-C,* ***(f)*** *C-C,* ***(g)*** *A-MA,* ***(h)*** *A-MB,* ***(i)*** *B-MA,* ***(j)*** *B-MB,* ***(k)*** *C-MA,* ***(l)*** *C-MB,* ***(m)*** *MA-MA,* ***(n)*** *MA-MB, and* ***(o)*** *MB-MB in butanoyl-chitosan obtained from atomistic (black) and CG (red) simulations.*

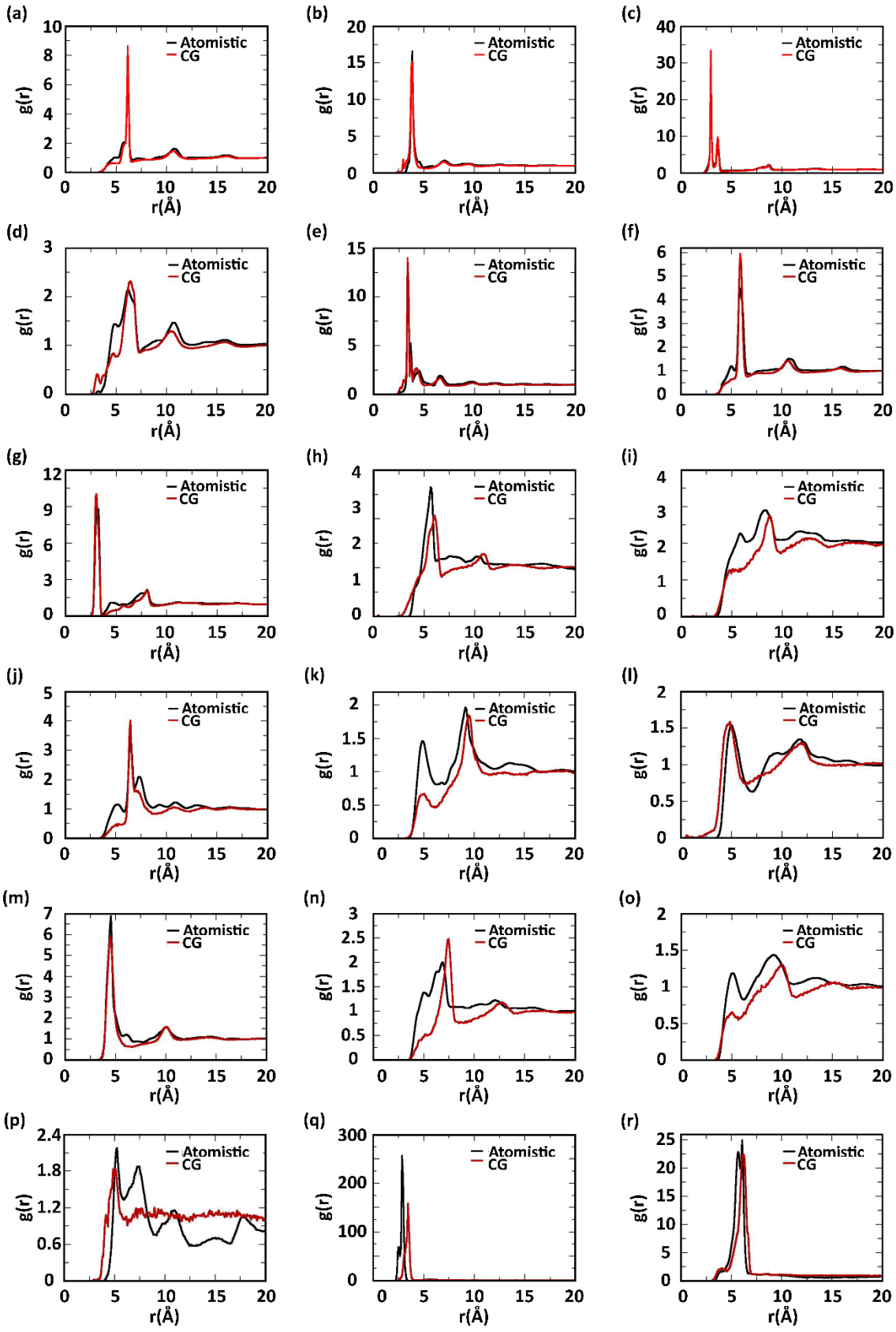
(a)
(b)
(c)
(d)
(e)
(f)
(g)
(h)
(i)
(j)
(k)
(l)
(m)
(n)
(o)
(p)
(q)
(r)
Atomistic
CG
g(r)
r(Å)

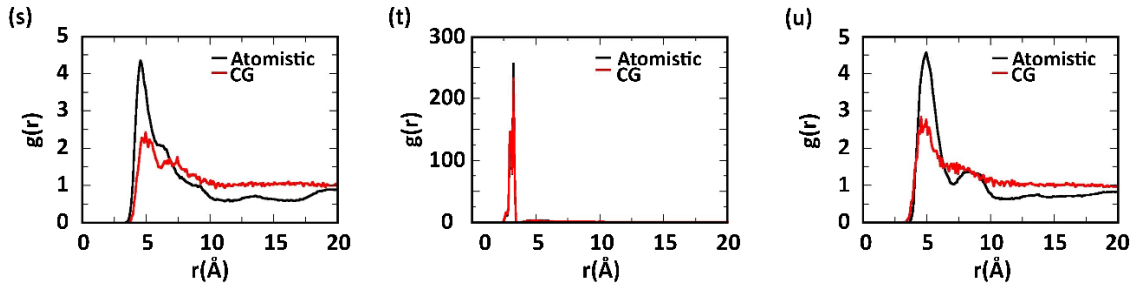


***Figure S3.*** *RDFs of the distance between CG beads* ***(a)*** *A-A,* ***(b)*** *A-B,* ***(c)*** *A-C,* ***(d)*** *B-B,* ***(e)*** *B-C,* ***(f)*** *C-C,* ***(g)*** *A-MA,* ***(h)*** *A-MB,* ***(i)*** *A-MC,* ***(j)*** *B-MA,* ***(k)*** *B-MB,* ***(l)*** *B-MC,* ***(m)*** *C-MA,* ***(n)*** *C-MB,* ***(o)*** *C-MC,* ***(p)*** *MA-MA,* ***(q)*** *MA-MB,* ***(r)*** *MA-MC,* ***(s)*** *MB-MB,* ***(t)*** *MB-MC, and* ***(u)*** *MC-MC in heptanoyl-chitosan obtained from atomistic (black) and CG (red) simulations.*

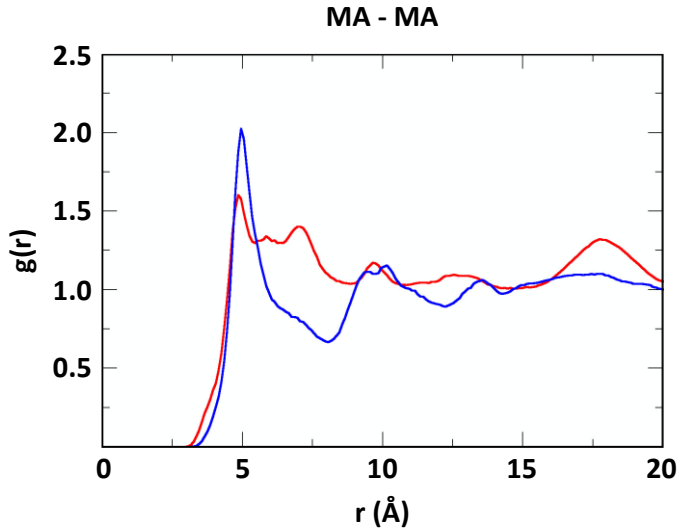


***Figure S4.*** *RDFs between MA-MA beads in two independent atomistic simulations of butanoyl-chitosan with* $\chi_{But}$ *= 32%.*

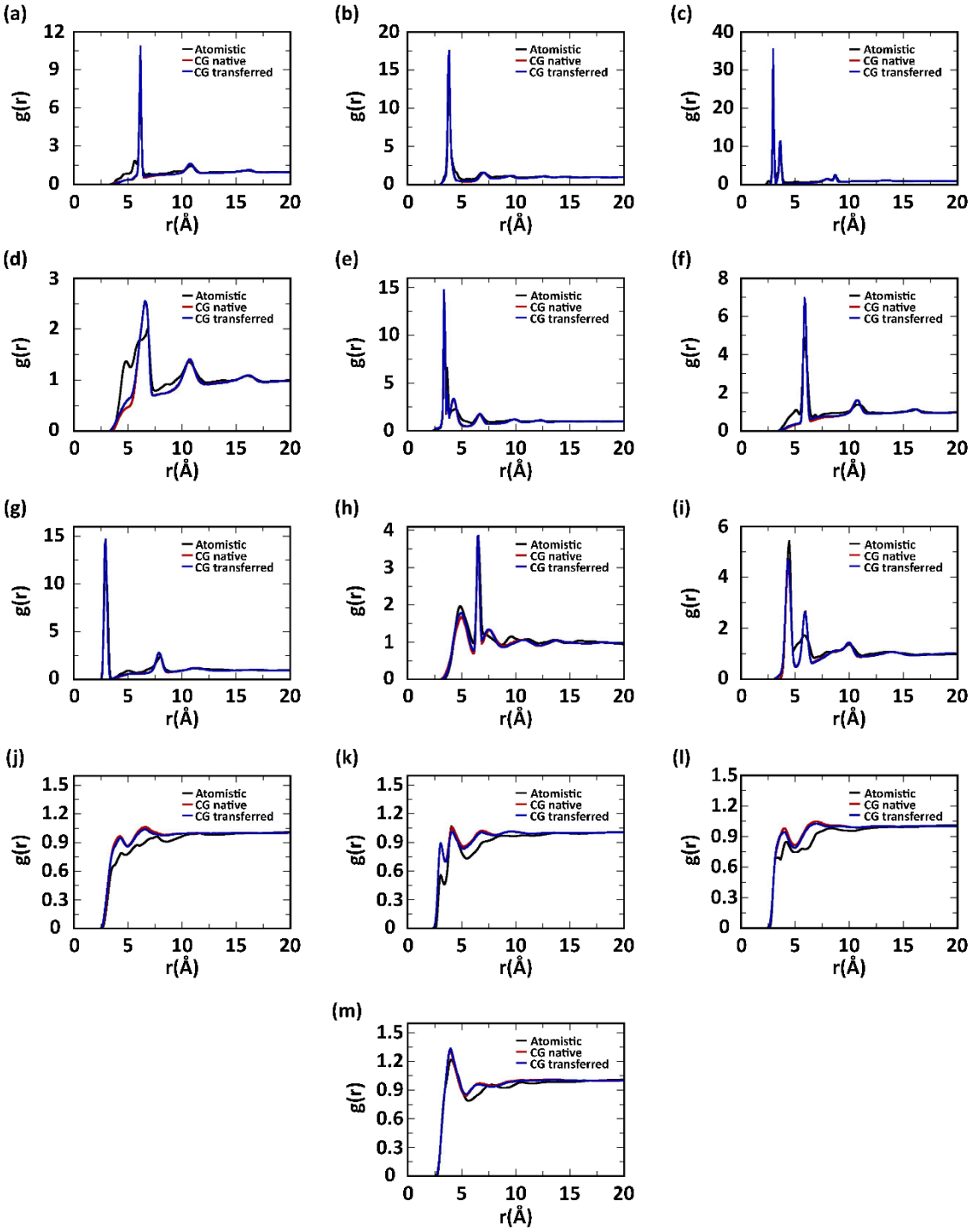


***Figure S5.*** *RDFs of the distance between CG beads* ***(a)*** *A-A,* ***(b)*** *A-B,* ***(c)*** *A-C,* ***(d)*** *B-B,* ***(e)*** *B-C,* ***(f)*** *C-C,* ***(g)*** *A-M,* ***(h)*** *B-M,* ***(i)*** *C-M,* ***(j)*** *A-WAT,* ***(k)*** *B-WAT,* ***(l)*** *C-WAT, and* ***(m)*** *M-WAT in acetyl-chitosan obtained with interaction potentials of atomistic system with* $\chi_{Ac}$ *= 32% (black), native CG system at* $\chi_{Ac}$ *= 32% (red), or transferred from a CG system with* $\chi_{Ac}$ *= 16% to a CG system with* $\chi_{Ac}$ *= 32% (blue).*

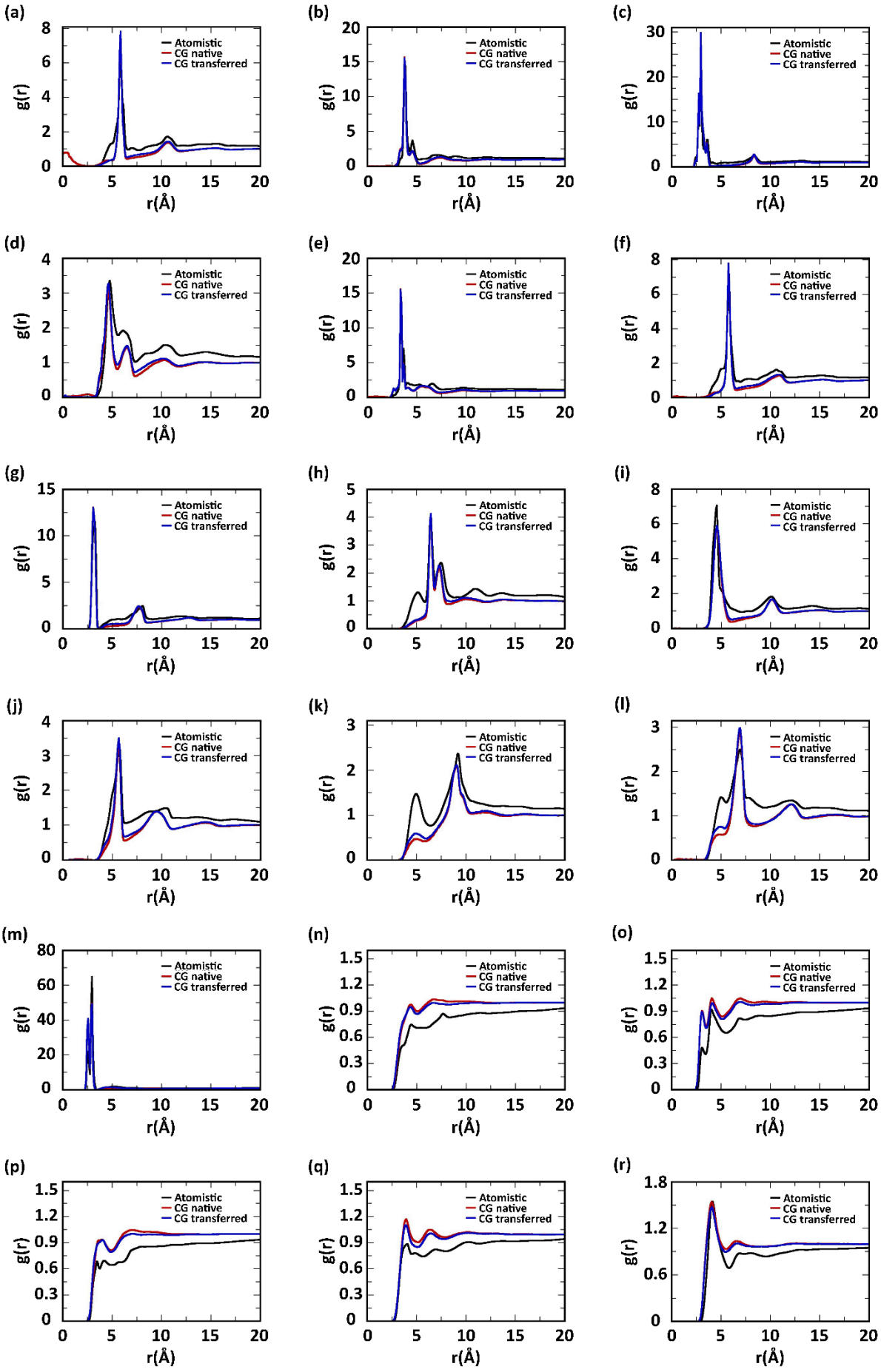
(a)
(b)
(c)
(d)
(e)
(f)
(g)
(h)
(i)
(j)
(k)
(l)
(m)
(n)
(o)
(p)
(q)
(r)
Atomistic
CG native
CG transferred
g(r)
r(Å)

***Figure S6.*** *RDFs of the distance between CG beads* ***(a)*** *A-A,* ***(b)*** *A-B,* ***(c)*** *A-C,* ***(d)*** *B-B,* ***(e)*** *B-C,* ***(f)*** *C-C,* ***(g)*** *A-MA,* ***(h)*** *B-MA,* ***(i)*** *C-MA,* ***(j)*** *A-MB,* ***(k)*** *B-MB,* ***(l)*** *C-MB,* ***(m)*** *MA-MA,* ***(n)*** *A-WAT,* ***(o)*** *B-WAT,* ***(p)*** *C-WAT,* ***(q)*** *MA-WAT, and* ***(r)*** *MB-WAT in butanoyl-chitosan obtained with interaction potentials of atomistic system with* $\chi_{But}$ *= 32% (black), native CG system at* $\chi_{But}$ *= 32% (red), or transferred from a CG system with* $\chi_{But}$ *= 16% to a CG system with* $\chi_{But}$ *= 32% (blue).*

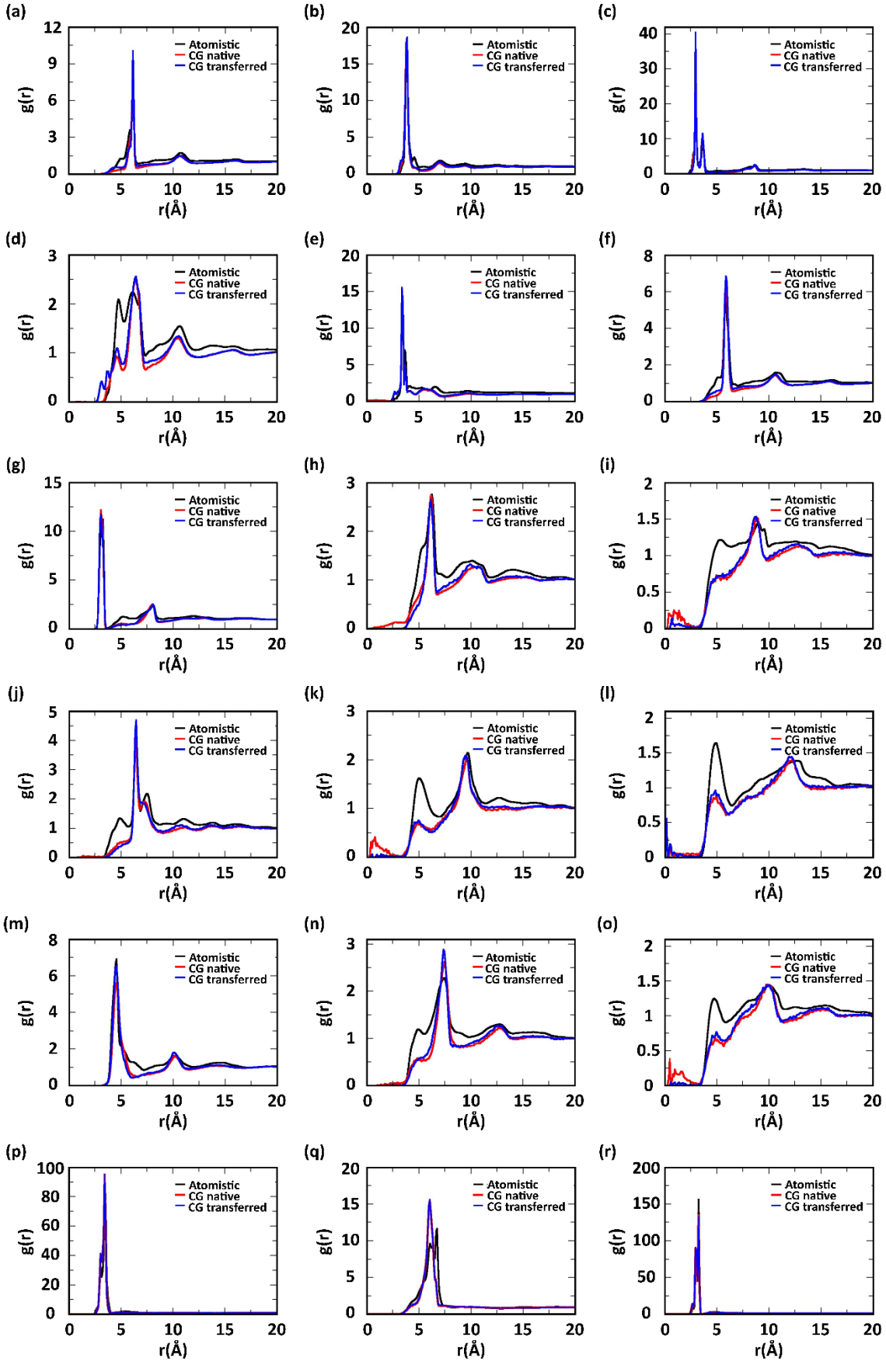
(a)
(b)
(c)
(d)
(e)
(f)
(g)
(h)
(i)
(j)
(k)
(l)
(m)
(n)
(o)
(p)
(q)
(r)
Atomistic
CG native
CG transferred
g(r)
r(Å)

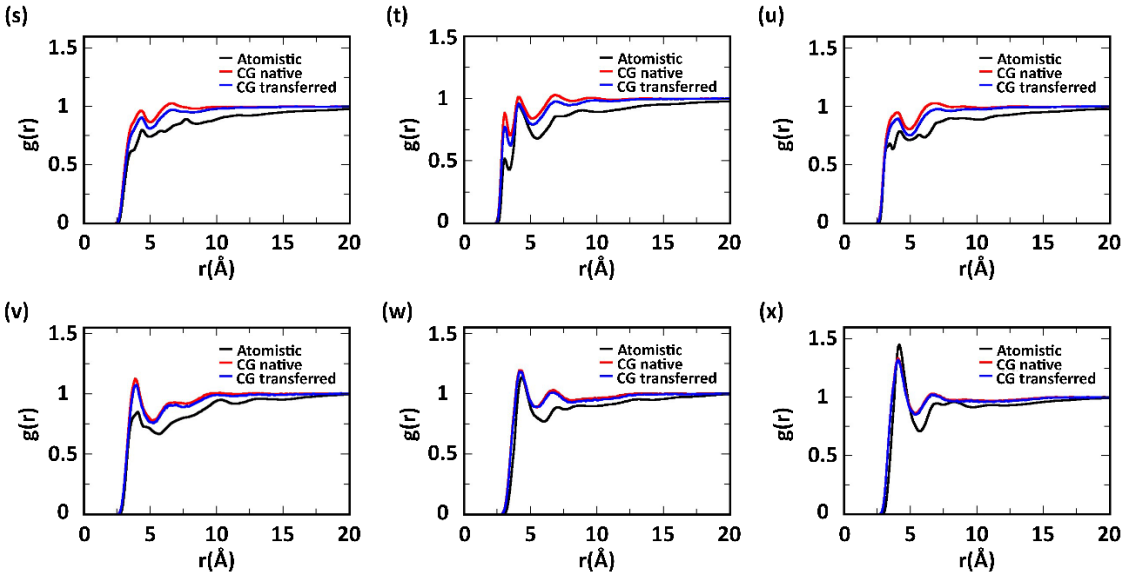


***Figure S7.*** *RDFs of the distance between CG beads* ***(a)*** *A-A,* ***(b)*** *A-B,* ***(c)*** *A-C,* ***(d)*** *B-B,* ***(e)*** *B-C,* ***(f)*** *C-C,* ***(g)*** *A-MA,* ***(h)*** *A-MB,* ***(i)*** *A-MC,* ***(j)*** *B-MA,* ***(k)*** *B-MB,* ***(l)*** *B-MC,* ***(m)*** *C-MA,* ***(n)*** *C-MB,* ***(o)*** *C-MC,* ***(p)*** *MA-MB,* ***(q)*** *MA-MC,* ***(r)*** *MB-MC,* ***(s)*** *A-WAT,* ***(t)*** *B-WAT,* ***(u)*** *C-WAT,* ***(v)*** *MA-WAT,* ***(w)*** *MB-WAT, and* ***(x)*** *MC-WAT in heptanoyl-chitosan obtained with interaction potentials of atomistic system with* $\chi_{Hep}$ *= 16% (black), native CG system at* $\chi_{Hep}$ *= 16% (red), or transferred from a CG system with* $\chi_{Hep}$ *= 8% to a CG system with* $\chi_{Hep}$ *= 16% (blue).*

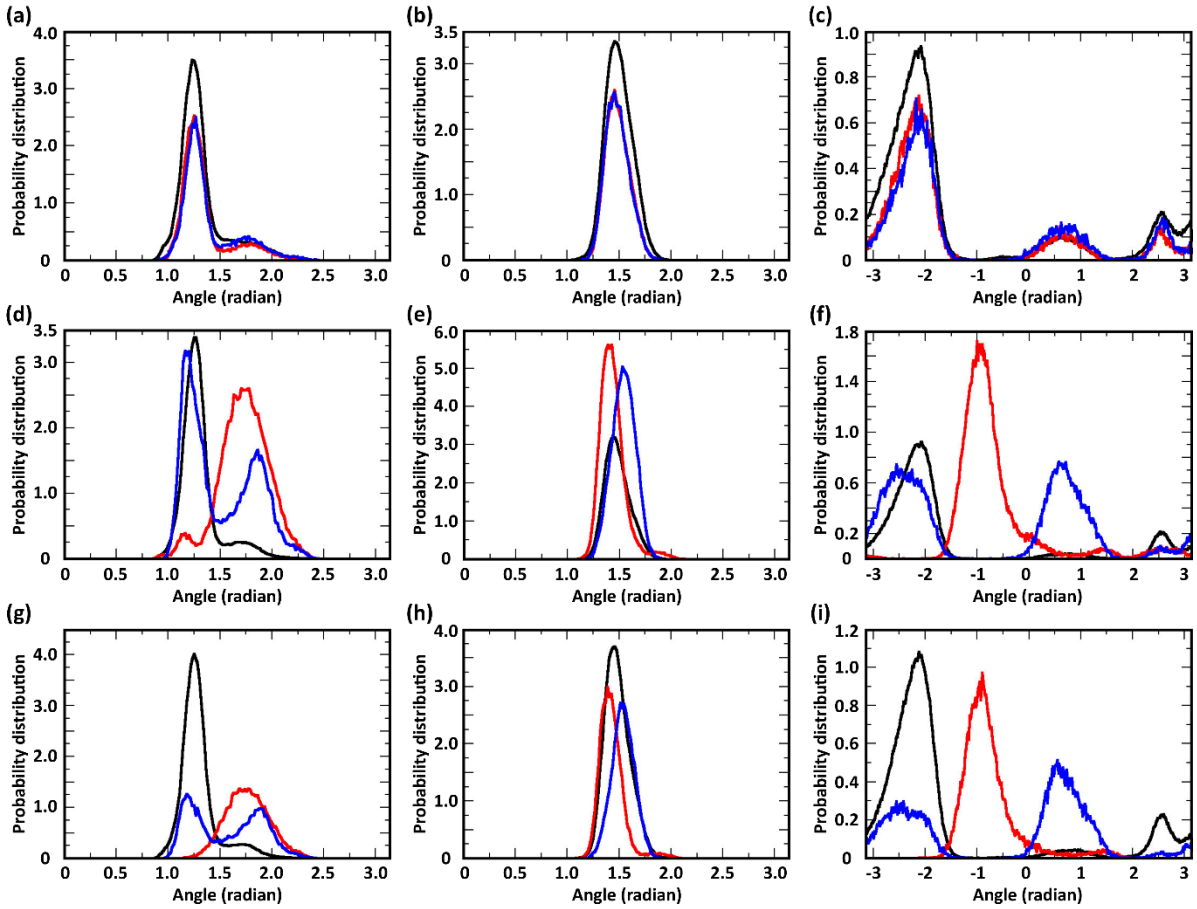


***Figure S8.*** *Angle distributions obtained for the glycosidic links between unsubstituted glucosamine monomers (black), at the non-reducing side of the substitution (red), and the reducing side of the substitutions (blue) via atomistic simulations of* ***(a)*** *BAC,* ***(b)*** *BCA, and* ***(c)*** *BACB for acetyl-chitosan;* ***(d)*** *BAC,* ***(e)*** *BCA, and* ***(f)*** *BACB for butanoyl-chitosan; and* ***(g)*** *BAC,* ***(h)*** *BCA, and* ***(i)*** *BACB for heptanoyl-chitosan.*

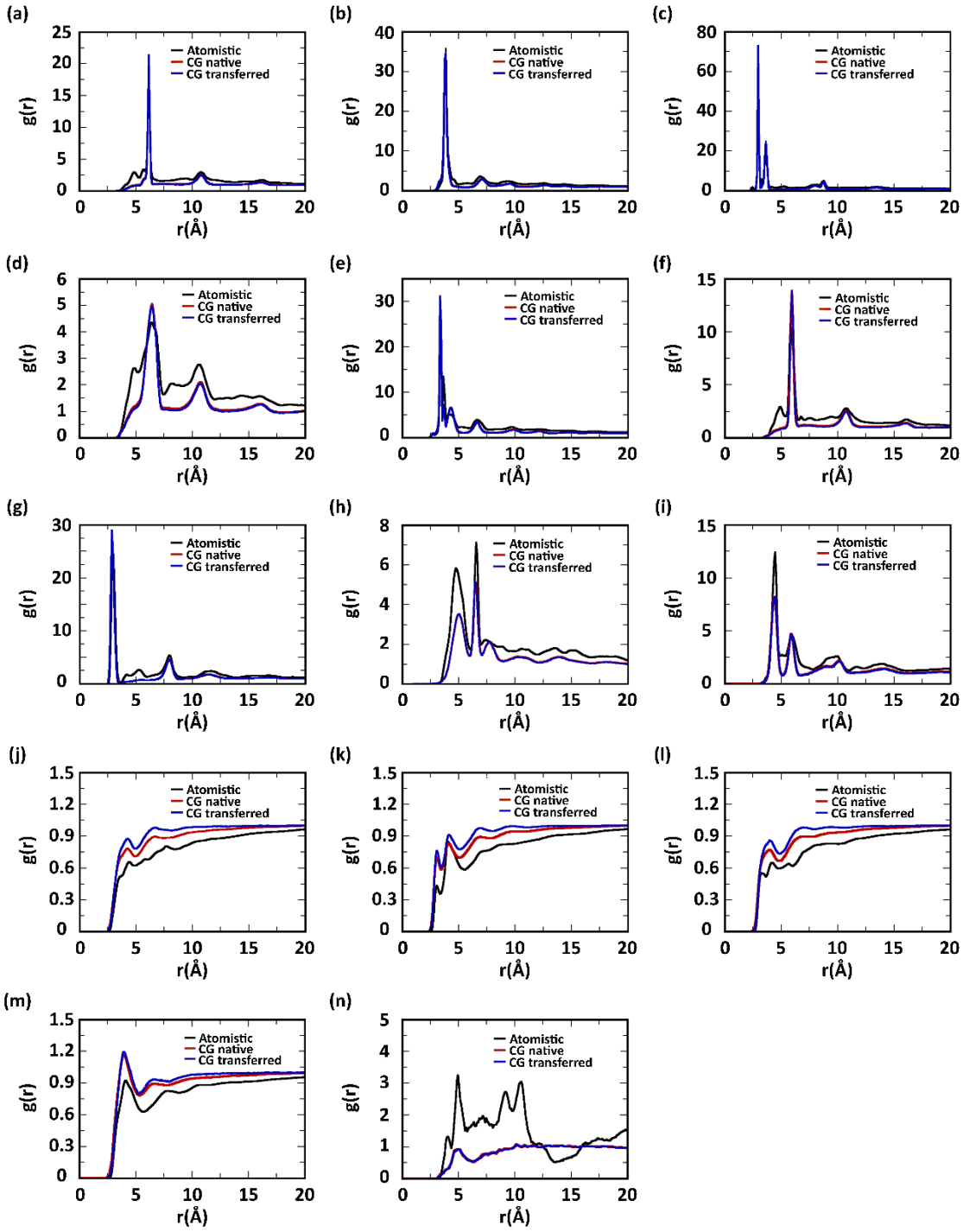


***Figure S9.*** *RDFs of the distance between CG beads* ***(a)*** *A-A,* ***(b)*** *A-B,* ***(c)*** *A-C,* ***(d)*** *B-B,* ***(e)*** *B-C,* ***(f)*** *C-C,* ***(g)*** *A-M,* ***(h)*** *B-M,* ***(i)*** *C-M,* ***(j)*** *A-WAT,* ***(k)*** *B-WAT,* ***(l)*** *C-WAT,* ***(m)*** *M-WAT, and* ***(n)*** *M-M in acetyl-chitosan obtained with interaction potentials of diluted atomistic (black) or native CG (red) systems, or transferred from concentrated (water-to-monomer ratio of 12) to diluted (water-to-monomer ratio of 32) CG systems (blue).*

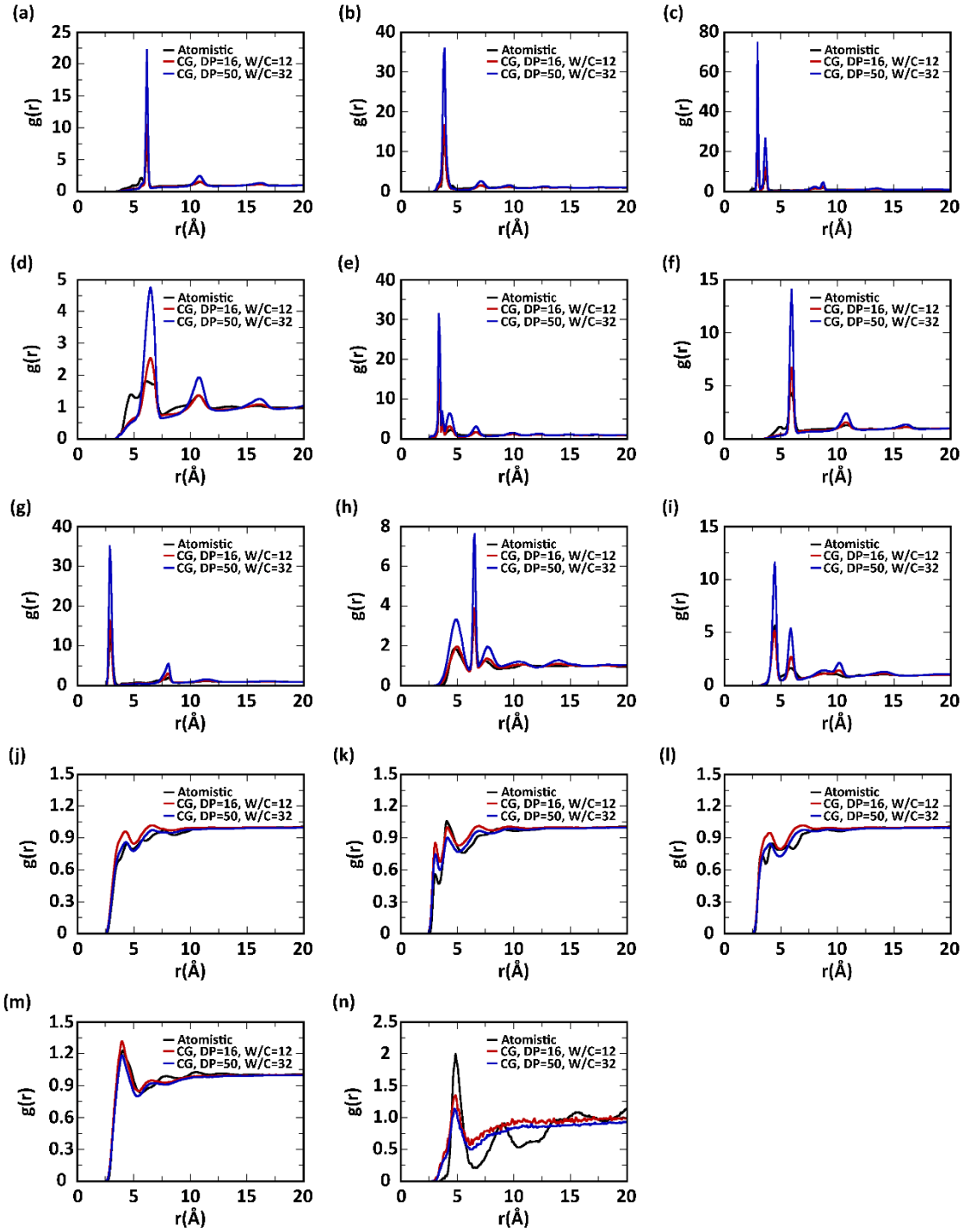


***Figure S10.*** *RDFs of the distance between CG beads* ***(a)*** *A-A,* ***(b)*** *A-B,* ***(c)*** *A-C,* ***(d)*** *B-B,* ***(e)*** *B-C,* ***(f)*** *C-C,* ***(g)*** *A-M,* ***(h)*** *B-M,* ***(i)*** *C-M,* ***(j)*** *A-WAT,* ***(k)*** *B-WAT,* ***(l)*** *C-WAT,* ***(m)*** *M-WAT, and* ***(n)*** *M-M in diluted (water-to-monomer ratio of 32) acetyl-chitosan with DP = 16 at atomistic (black) or CG (red) resolution, or DP = 50 at CG resolution (blue).*

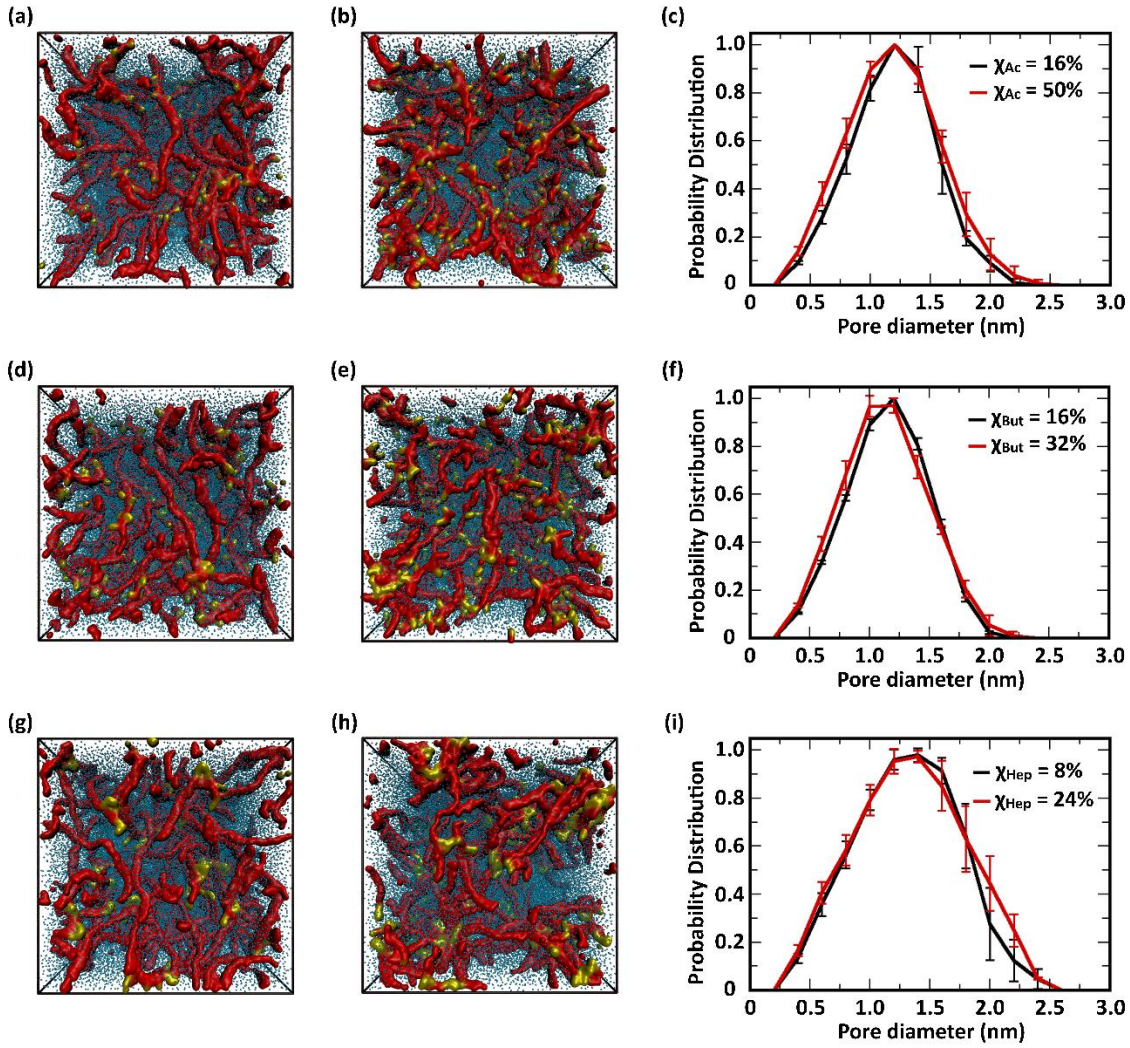


***Figure S11.*** *Simulation snapshots of networks containing 20 chitosan chains of DP = 50 and 50 water molecules/monomer, and modified with acetyl groups at* ***(a)*** $\chi_{Ac}$ *= 16% and* ***(b)*** $\chi_{Ac}$ *= 50%, and* ***(c)*** *corresponding pore-size distributions; butanoyl groups at* ***(d)*** $\chi_{But}$ *= 16% and* ***(e)*** $\chi_{But}$ *= 32% , and* ***(f)*** *corresponding pore-size distributions; heptanoyl groups at* ***(g)*** $\chi_{Ac}$ *= 8% and* ***(h)*** $\chi_{Ac}$ *= 24%, and* ***(i)*** *corresponding pore-size distributions. The chitosan backbone beads (A, B, and C) are in red, modification beads (M, MA, MB, and MC) are in yellow, and water beads are in blue. All modification groups were distributed in blocks of four on the chitosan chains.*

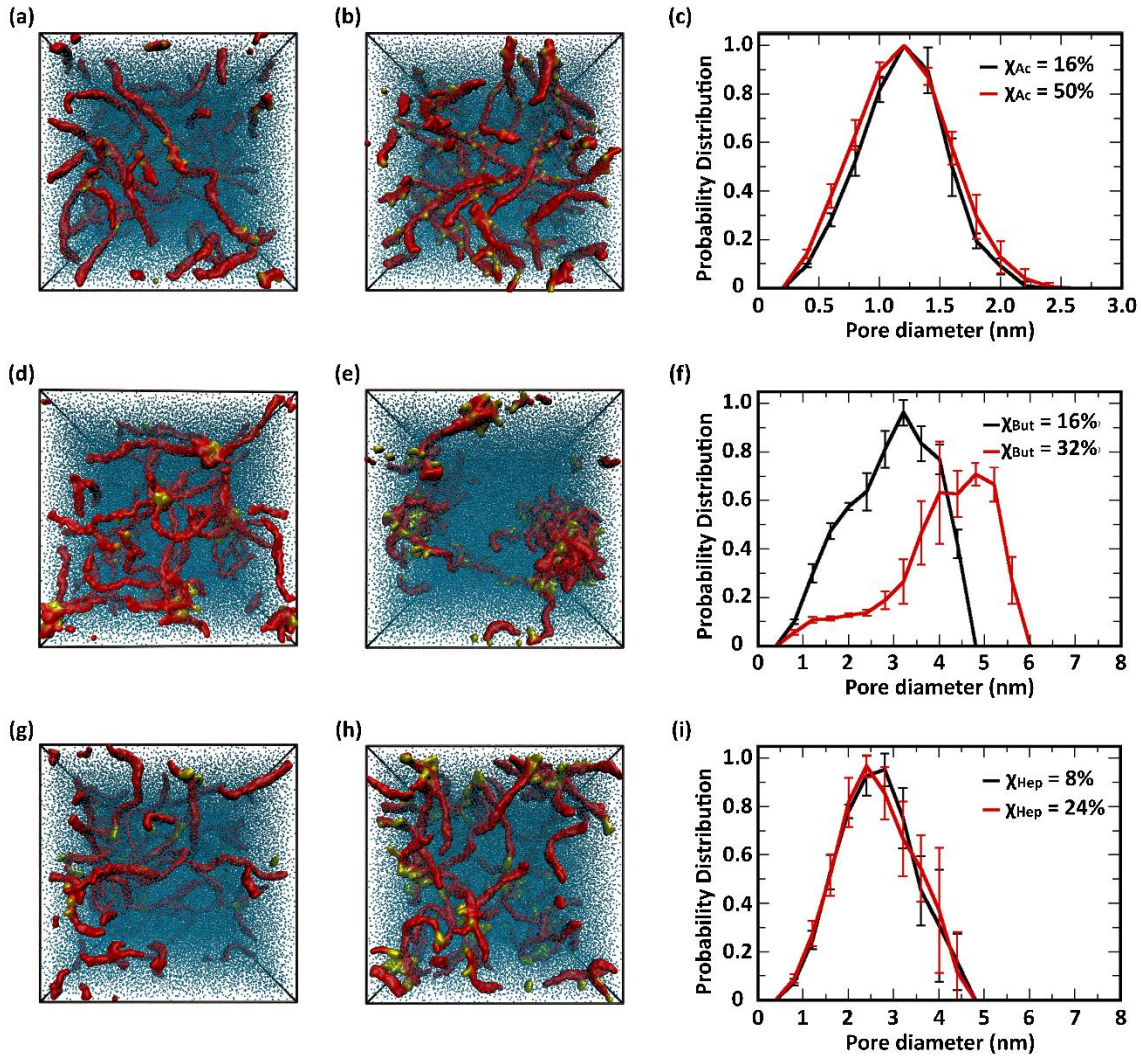


***Figure S12.*** *Simulation snapshots of networks containing 50 chitosan chains of DP = 100 and water-to-monomer ratio of 32, and modified with acetyl groups at* ***(a)*** $\chi_{Ac}$ *= 16% and* ***(b)*** $\chi_{Ac}$ *= 50%, and* ***(c)*** *corresponding pore-size distributions; butanoyl groups at* ***(d)*** $\chi_{But}$ *= 16% and* ***(e)*** $\chi_{But}$ *= 32%, and* ***(f)*** *corresponding pore-size distributions; heptanoyl groups at* ***(g)*** $\chi_{Ac}$ *= 8% and* ***(h)*** $\chi_{Ac}$ *= 24%, and* ***(i)*** *corresponding pore-size distributions. The chitosan backbone beads (A, B, and C) are in red, modification beads (M, MA, MB, and MC) are in yellow, and water beads are in blue. All modification groups were distributed in blocks of four on the chitosan chains.*

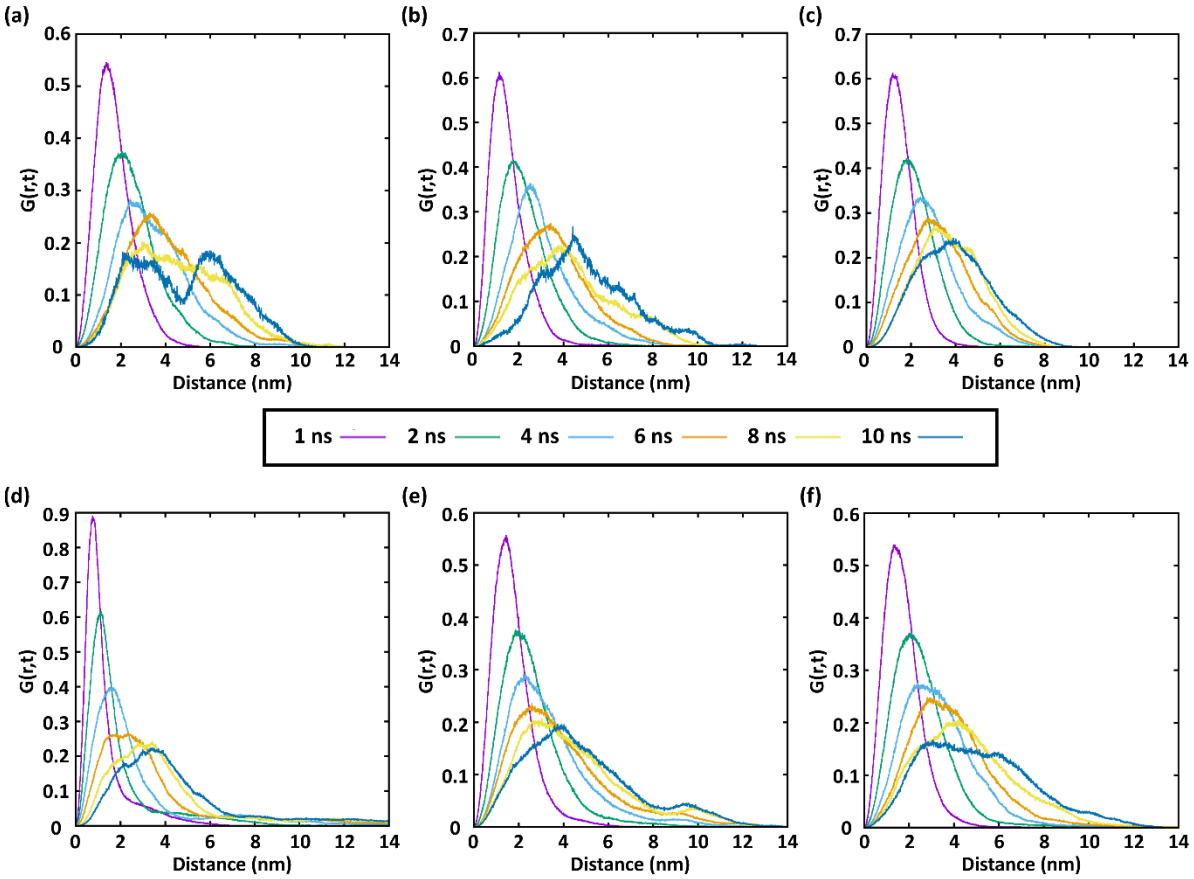


***Figure S13.*** *Van Hove functions for DOX in* ***(a)*** *acetyl-chitosan with* $\chi_{Ac}$ *= 16%,* ***(b)*** *acetyl-chitosan with* $\chi_{Ac}$ *= 50%,* ***(c)*** *butanoyl-chitosan with* $\chi_{But}$ *= 16%,* ***(d)*** *butanoyl-chitosan with* $\chi_{But}$ *= 32%,* ***(e)*** *heptanoyl-chitosan with* $\chi_{Hep}$ *= 8%, and* ***(f)*** *heptanoyl-chitosan with* $\chi_{Hep}$ *= 24%.*

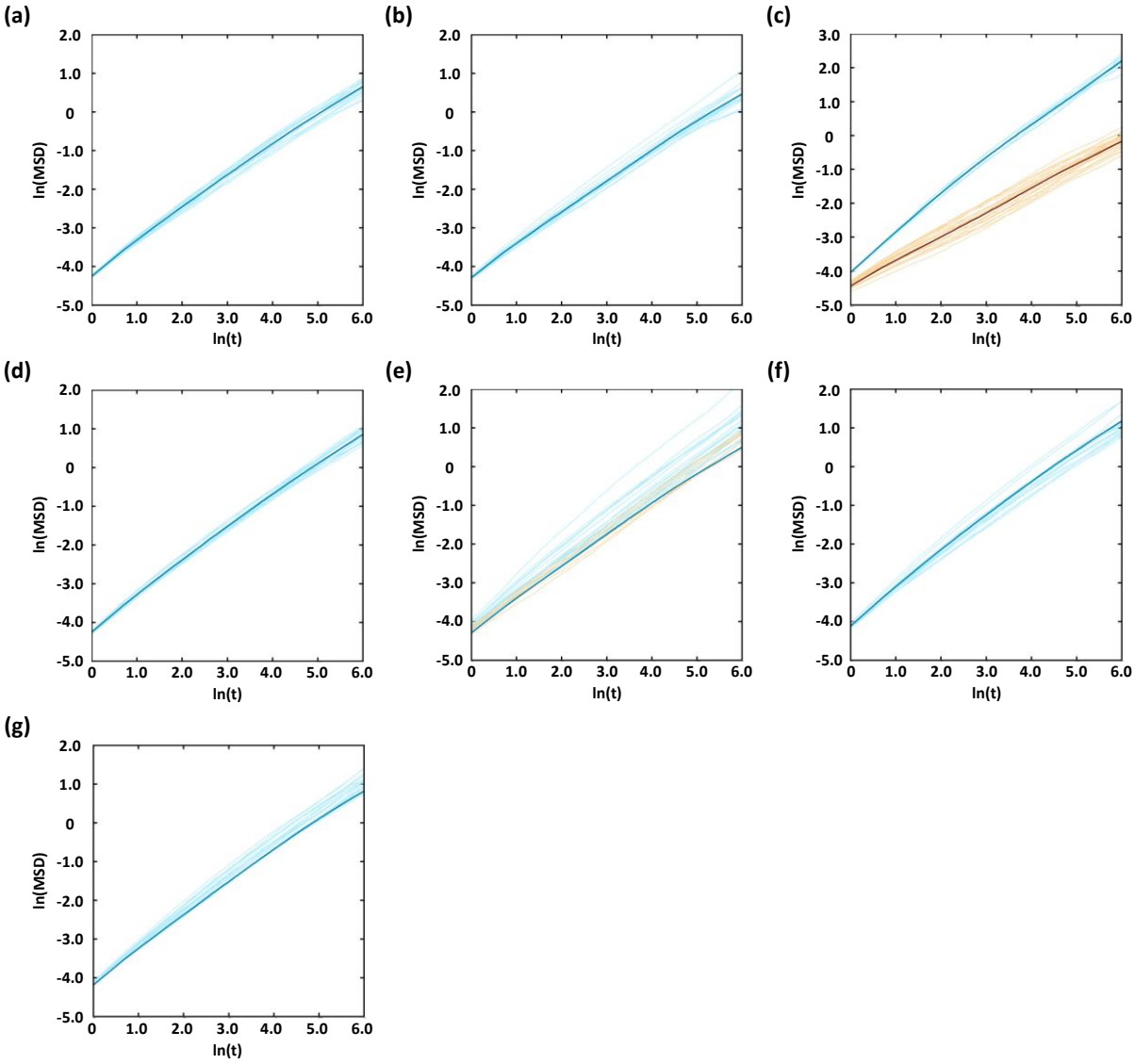


***Figure S14.*** *log-log plots of the MSD of individual Dox molecules in* ***(a)*** *acetyl-chitosan with* $\chi_{Ac}$ *= 16%,* ***(b)*** $\chi_{Ac}$ *= 50%,* ***(c)*** *butanoyl-chitosan with* $\chi_{But}$ *= 32%,* ***(d)*** *butanoyl-chitosan with* $\chi_{But}$ *= 16% and uniform distribution,* ***(e)*** *butanoyl-chitosan with* $\chi_{Ac}$ *= 16% and blocky distribution,* ***(f)*** *heptanoyl-chitosan with* $\chi_{Hep}$ *= 8%, and* ***(g)*** *heptanoyl- chitosan with* $\chi_{Hep}$ *= 24%.*